



AIAA 99-0327

**Suppression of Bluff-Body Stabilized
Pool Flames**

F. Takahashi and W. J. Schmoll
University of Dayton
Dayton, OH

V. M. Belovich
Air Force Research Laboratory
Wright-Patterson Air Force Base, OH

**37th AIAA Aerospace Sciences
Meeting and Exhibit
January 11-14, 1999 / Reno, NV**

SUPPRESSION OF BLUFF-BODY STABILIZED POOL FLAMES

Fumiaki Takahashi* and W. John Schmoll†
 University of Dayton Research Institute
 300 College Park, Dayton, Ohio 45469

Vincent M. Belovich‡
 Air Force Research Laboratory
 Wright-Patterson Air Force Base, Ohio 45433

ABSTRACT

The suppression mechanisms of a nonpremixed flame stabilized behind a backward-facing step in a wind tunnel have been studied using a gaseous fire-extinguishing agent (Halon 1301, bromotrifluoromethane) into the airflow. Methane or JP-8 jet fuel was used to simulate a pool fire behind a clutter in the aircraft engine nacelle. The characteristic mixing time (τ_{exp}) in the recirculation zone in the wake was measured by impulsively injecting salt water mist into the airflow and by determining a time constant for the exponential decay of the sodium D-line emission at high temperatures. For three different step heights (h_s) and various mean inlet air velocities (U_{a0}), τ_{exp} linearly depended on h_s/U_{a0} . For both methane and JP-8 fuels under relatively high air velocities, the dependence of the critical agent mole fraction at extinction on the injection period is predictable using the characteristic mixing time and the minimum agent mole fraction, which is a fuel property measurable by a steady-state cup-burner method.

INTRODUCTION

A recirculation zone formed behind a clutter in the aircraft engine nacelle, which encases the engine compressor, combustors and turbine, can stabilize fires under over-ventilated conditions [1-7, 9, 10]. The fuel sources are leaking jet-fuel and hydraulic-fluid lines that can feed the fire in the form of a spray or pool. Suppression occurs when a critical concentration of agent is transported to the fire. As currently-used Halon 1301 (CF_3Br) fire extinguishant is replaced with a possibly less effective agent, the amount of replacement agent required for fire suppression over a range of

operating conditions must be determined. Hence, it is not known whether or not the flame extinguishing data using conventional cup burner or counterflow diffusion flame methods [7, 12-14] can characterize the bluff-body stabilized flames.

The objectives of this study are: (1) determine difficult-to-extinguish cases by a parametric investigation, (2) gain a better understanding of the flame stabilization and suppression mechanisms of bluff-body stabilized flames, and (3) develop a phenomenological model that can be integrated into computational fluid dynamics models for predicting fires and their suppression.

In the previous paper [15], the critical suppression limits of step-stabilized methane flames were reported for two different step heights and various air velocities using Halon 1301 as the baseline agent. In this paper, the new suppression limit data are reported for additional step height and air velocity, and the JP-8 liquid fuel pool flame was used as well. More importantly, the characteristic mixing time in the recirculation zone was measured for the first time to gain a better understanding of the fundamental mechanisms of fire suppression.

EXPERIMENTAL TECHNIQUES

The experimental apparatus (Fig. 1) is essentially the same as reported in the previous paper [15] with some modification for the liquid fuel. The apparatus consists of the fuel, air, and agent supply systems, a horizontal small-scale wind tunnel, and a combustion product scrubber. Methane issues upward at a mean velocity of 0.7 cm/s (flow rate: 10 l/min) from a porous plate ($150 \times 150 \times 12.7$ -mm thickness, stainless steel) placed downstream of a backward-facing step (height [h_s]: 32 mm, 64 mm, or 96 mm) in the test section (154×154 -mm² cross-section, 77-cm length). The porous plate is lowered about 6.4 mm in the case of the liquid fuel pool configuration. A liquid fuel (JP-8) supply and

* Research Engineer, Research Institute, Senior Member AIAA

† Associate Research Physicist, Research Institute

‡ Mechanical Engineer, Propulsion Sciences and Advanced Concept Division, Member AIAA

Copyright © 1999 by the authors. Published by the American Institute of Aeronautics and Astronautics, Inc. with permission.

leveling system consists of a fuel tank (volume: 7.6 l), a liquid fuel tubing connecting the fuel tank and the porous plate housing, and a pressure tap tubing from the top of the test section to the other end emerging into the fuel tank sight glass. By adjusting the height of the tip of the pressure tap tubing in the fuel tank sight glass, the liquid level in the test section can be controlled automatically.

The airflow is regulated by passing through honeycombs, a diffuser, mesh screens (#100), a contraction nozzle, and a turbulence generating perforated plate (33% opening, 2.4 mm-dia. holes). The turbulence level in the wind tunnel is typically ~6%. The mean air velocities at the test section inlet (U_{a0}) and the step (U_{as}) are calculated by dividing the volumetric flow rate by the cross-sectional areas of the full test section and the air passage above the step, respectively.

The agent supply system, which is similar to that of Hamins et al. [7, 9], consists of a (liquid) agent reservoir (3.8 l), two connected gaseous agent storage vessels (38 l each), and a computer-controlled solenoid valve. The gaseous agent was injected impulsively into the air ~1 m upstream of the flame. Uniform agent dispersion into the airstream was achieved by injecting the agent radially into a reduced diameter (108 mm) section of the air passage through 16 6.4-mm-dia. holes in a 25.4-mm-o.d. closed-end tube. The mesh screens and a perforated plate downstream ensure complete agent-air mixing prior to entering the flame zone. The storage volume, including two pressure vessels and associated plumbing, is 79.9 l. The agent temperature and pressure in the second storage vessel are measured with a type-T thermocouple and a pressure transducer. The amount of injected agent is controlled by varying the initial pressure and the time period that the valve is open and determined from the difference between the initial and final pressures in the storage vessel using the ideal-gas equation of state. The mean volumetric agent concentration is determined by dividing the mean agent flow rate ([volume]/[injection period]) by the airflow rate.

The cyclone-type scrubber is attached to the exit of the test section to remove acidic gases (HF) by water sprays from eight pressure-swirl atomizers on the top plate. The gases are exhausted through the central tube and the water is collected in a drain tank. An air-driven ejector is attached to the scrubber exit to reduce the backpressure and adjust the pressure of the test section to atmospheric.

The extinction limit experiment is conducted as follows. First, a stable flame is established for a fixed mean airflow velocity, and then the agent is injected for a particular storage vessel pressure and an injection period. The agent injection test is repeated 20 times to

determine the probability of extinction. Then either the storage vessel pressure or injection period is varied step-wise and repeat the experiment. The extinction condition is confirmed at a probability of 90% chosen arbitrary.

The characteristic mixing time is measured as follows. A fine-mist spray of saturated salt (NaCl)-water solution is injected impulsively (~1 s) into the air supply plenum before a honeycomb flow straightener using an artist's airbrush. The emission by flame reaction of sodium (D-line, 589 nm) in the high temperature recirculation zone is collected by a lens and passed through an interference filter, and detected by a photomultiplier. The converted electronic signal is conditioned by a low-pass filter (cutoff frequency: typically 20 Hz) and an amplifier. The emission intensity reaches a maximum value during the pulsed injection and then decays exponentially based on the turbulent material exchange between the recirculation zone and the free air stream based on the first-order differential equation:

$$C = -\tau(dC/dt) \quad (1)$$

where C is the concentration of sodium, t is the elapsed time, and τ is the time constant. The solution for the equation is

$$(C/C_0) = \exp(-t/\tau) \quad (2)$$

where C_0 is the initial concentration. Figure 2 shows a typical signal trace of the normalized sodium emission intensity. The characteristic mixing time (τ_{exp}), or residence time, in the recirculation zone is determined from the slope of the plot. The measurement is repeated typically 20 times and averaged.

RESULTS AND DISCUSSION

Figure 3 shows the measured characteristic mixing time for three different step heights. At low air velocities ($U_{a0} < 3$ m/s) and long mixing times ($\tau_{exp} > 0.5$ s), the measurement was prohibited due to high-amplitude, low-frequency noises. For a given h_s , τ_{exp} decreased monotonically with an increased U_{a0} . For a fixed U_{a0} , τ_{exp} increased proportionally with h_s . Thus, the data points were plotted against h_s/U_{a0} in Fig.4. A good linear correlation (the coefficient of determination $R^2 = 0.943$) was obtained as

$$\tau_{exp} = 22.79 (h_s/U_{a0}) \quad (3)$$

in the range of $U_{a0} > 3$ m/s and $\tau_{exp} < 0.5$ s.

In the previous paper [15], the critical agent mole fraction at suppression (X_c) of methane flames as a

function of agent injection period (Δt) at different mean air velocities was reported for two different step heights ($h_s = 32$ mm and 64 mm). Figure 5 shows the new results for $h_s = 96$ mm, indicating the similar trend; i.e., as Δt was increased for a given U_{a0} , X_c decreased monotonically. As the step height was increased, the suppression-limit curves generally shifted upward (and rightward); namely, for given U_{a0} and Δt , X_c increased and for a fixed U_{a0} and X_c , Δt increased. For a low U_{a0} , large X_c and Δt were required to suppress the flame. As pointed out in the previous paper [15], for $U_{a0} = 0.3$ m/s, the extinction limit curve exceeded the design condition for the current halon fire-extinguishing system in the engine nacelle, which requires to achieve 6% agent concentration everywhere for at least 0.5 s. At this air velocity, the extinction limit curve for $h_s = 96$ mm was even farther shifted upward and rightward.

For higher air velocities, there was a minimum agent mole fraction below which no extinction occur even at long injection periods. The value determined previously [15] is $X_c = 0.025$ and applies to all step heights. This agent concentration threshold must be a property of the type of fuel and is roughly consistent with the minimum agent concentration of $\sim 3\%$ obtained using a cup burner and counterflow diffusion flames at a low strain rate (50 s⁻¹) [7, 8]. Furthermore, there existed a minimum injection period, below which the flame could not be extinguished even at high agent concentrations: $\Delta t \approx 0.05$ s for $h_s = 32$ mm, $\Delta t \approx 0.1$ s for $h_s = 64$ mm [15], and $\Delta t \approx 0.15$ s for $h_s = 96$ mm.

In the previous paper [15], it was shown that the suppression-limit curves for high air velocity cases can be explained by the turbulent mixing between the recirculation zone and the free air stream using the following equation derived by Hamins et al [10] based on a phenomenological model for a well-stirred reactor developed by Longwell et al. [16]. It was assumed that the flame was stabilized in the recirculation zone downstream of the baffle. To extinguish the flame, the agent mole fraction in the recirculation zone had to obtain a critical value (X_∞). Complete mixing of the agent in the

$$X_c(\Delta t) = \frac{X_\infty(\Delta t \gg \tau)}{1 - e^{(-\Delta t/\tau)}} \quad (4)$$

recirculation zone was instantaneous.

where τ is the characteristic mixing time for entrainment into the recirculation zone. For long injection period, $X_c \approx X_\infty$. For short injection period, large free stream agent concentrations are required to obtain extinction.

Figure 6 shows the extinction limits for $U_{a0} = 7.1$ m/s for three different step heights and theoretical curves using Eq. (4) with $X_\infty = 0.025$ and τ_{exp} from Eq. (3). The

theoretical curves showed a general trend obtained experimentally; the curves for the measured τ_{exp} generally follow the data points for different step heights. Surprisingly, the measured τ_{exp} 's for $h_s = 32$ mm, 64 mm 96 mm are almost exactly the same as arbitrarily chosen in the previous paper [15].

Figure 7 shows the replot of the data points using the normalized agent injection period ($\Delta t/\tau_{exp}$) with a theoretical curve of Eq. (4) with $X_\infty = 0.025$ and τ_{exp} from Eq. (3). Because τ_{exp} is proportional to h_s/U_{a0} , a plot using h_s/U_{a0} in abscissa showed the same trend [15]. The data points for three different step heights nearly collapsed into a single curve, and can be predicted theoretically.

From a practical point of view, the total amount of agent delivered under a given air flow rate condition is important. Figure 8 shows a re-plot of the data, presented in Fig. 5, in which the total agent mass required to extinguish the flame (m_{total}) is plotted as a function of the critical agent mole fraction. Figure 9 shows the minimum total agent mass ($m_{total, min}$) determined from Fig. 8, together with the previous result [15], plotted against the mean air velocity at the step. Here, U_{as} was used because the flame detachment process was controlled by the local velocity rather than the global U_{a0} . As U_{as} was increased, $m_{total, min}$ increased proportionally, and the transition from regime I (rim-attached flame) to II (wake-stabilized flame) occurs as the curves tend to level off. A larger step possessing a larger recirculation zone volume requires a larger agent mass to achieve the same agent concentration in the recirculation zone to extinguish the flame.

Figure 10 shows the suppression-limit curves for the JP-8 fuel flames for two different step heights and two air velocities, corresponding to regimes I and II. The theoretical curves of Eq. (4) with $X_\infty = 0.04$ and τ_{exp} from Eq. (3) are included in the figure as well. The JP-8 results showed a trend similar to that of methane except for the higher X_∞ . The theoretical curves show the experimental trend not only for the high air velocity but also for the low velocity case in regime I although there is a larger scatter in the experimental data points. The result suggests that there is a potential for a universal treatment of the data trend applicable to various fuels and geometric configurations.

Unlike gaseous fuel experiments, the rate of vaporization of a liquid fuel and, in turn, the fuel flow rate varies depending on the heat transfer from the flame to the fuel surface. As a result, the appearance of the flame depends on the air flow rate, which changes the heat transfer conditions, in addition to the differences between the rim-attached and wake-stabilized flames. However, the effect of the fuel flow rate appears to be

relatively small because of the nonpremixed flame characteristics. Furthermore, the JP-8 flame produced significant amount of soot, which was quickly accumulated on the windows and inner walls of the test section, making the experiment more difficult.

CONCLUSIONS

The extinction limits of nonpremixed methane or JP-8 flames stabilized by a backward-facing step in an airstream were reported using a gaseous fire-extinguishing agent (Halon 1301). The characteristic mixing time in the recirculation zone, measured by the sodium D-line emission decay, proportionally depends on h_s/U_{a0} . The measured data points of the critical agent mole fraction at extinction expressed as a function of the agent injection period normalized by the characteristic mixing time collapsed into a single curve, which closely follows the curve derived theoretically. The volume of the recirculation zone relates to the agent mass required to achieve the same agent concentration in the recirculation zone to extinguish the flame. The trend of the suppression limit curves is the same for methane and JP-8 fuel except the minimum agent mole fraction of $X_\infty = 0.025$, and 0.04 , respectively.

ACKNOWLEDGMENT

This research is part of the Department of Defense's Next-Generation Fire Suppression Technology Program, funded by the DoD Strategic Environmental Research and Development Program and the Air Force Research Laboratory, Propulsion Directorate, Propulsion Sciences and Advanced Concept Division, Wright-Patterson Air Force Base, Ohio, under Contract No. F33615-97-C-2719 (Technical Monitor: C. W. Frayne).

REFERENCES

1. Hirst, R., Farenden, P. J., and Simmons, R. F., "The Extinction of Fires in Aircraft Jet Engines—Part I, Small-Scale Simulation of Fires," *Fire Technology* 12: 266-289 (1976).
2. Hirst, R., Farenden, P. J., and Simmons, R. F., "The Extinction of Fires in Aircraft Jet Engines—Part II, Full-Scale Fire Tests," *Fire Technology* 13: 59-67 (1977).
3. Dyer, J. H., Marjoram, M. J., and Simmons, R. F., "The Extinction of Fires in Aircraft Jet Engines—Part III, Extinction of Fires at Low Air flows," *Fire Technology* 13: 126-138 (1977).
4. Dyer, J. H., Marjoram, M. J., and Simmons, R. F., "The Extinction of Fires in Aircraft Jet Engines—Part IV, Extinction of Fires by Sprays of Bromochlorodifluoromethane," *Fire Technology* 13: 223-230 (1977).
5. Moussa, N. A., "Effects of Clutter on Performance of Fire Suppression Agents in Aircraft Dry Bays and Engine Nacelles," Report prepared for Booz, Allen and Hamilton, Dayton, Ohio, April 1994.
6. Grosshandler, W. L., Gann, R. G., and Pitts, W. M., "Introduction," *Evaluation of Alternative In-Flight Fire Suppressants for Full-Scale Testing in Simulated Aircraft Engine Nacelles and Dry Bay Bays* (Grosshandler, W. L., Gann, R. G., and Pitts, W. M., eds.), NIST SP 861, National Institute of Standards and Technology, April 1994, pp. 1-12.
7. Hamins, A., Gmurczyk, G., Grosshandler, W., Rehwoldt, R. G., Vazquez, I., Cleary, T., Presser, C., and Seshadri, K., "Flame Suppression Effectiveness," *ibid.*, April 1994, pp. 345-465.
8. Hamins, A., Trees, D., Seshadri, K., and Chelliah, H. K., "Extinction of Nonpremixed Flames with Halogenated Fire Suppressants," *Combustion and Flame* 99: 221-230 (1994).
9. Hamins, A., Cleary, T., Borthwick, P., Gorchkov, N., McGrattan, K., Forney, G., Grosshandler, W., Presser, C., and Melton, L., "Suppression of Engine Nacelle Fires," *Fire Suppression System Performance of Alternative Agents in Aircraft Engine and Dry Bay Laboratory Simulations* (R. G. Gann, ed.), NIST SP 890: Vol. II, National Institute of Standards and Technology, Nov. 1995, pp.1-199.
10. Hamins, A., Presser, C., and Melton, L., "Suppression of a Baffle-Stabilized Spray Flame by Halogenated Agents," *Twenty-Sixth Symposium (International) on Combustion*, The Combustion Institute, 1996, pp. 1413-1420.
11. Gran, I. R., and Magnussen, B. F., "A Numerical Study of a Bluff-Body Stabilized Diffusion Flame. Part 1. Influence of Turbulence Modeling and Boundary Conditions," *Combustion Science and Technology* 119: 171-190 (1996).
12. Saso, Y., Saito, N., Liao, C., and Ogawa, Y., "Extinction of Counterflow Diffusion Flames with Halon Replacements," *Fire Safety Journal* 26: 303-326 (1996).
13. Liao, C., Saito, N., Saso, Y., and Ogawa, Y., "Flammability Limits of Combustible Gases and Vapors Measured by a Tubular Flame Method," *Fire Safety Journal* 27: 49-68 (1996).
14. Saito, N., Saso, Y., Liao, C., and Ogawa, Y., "Flammability Peak Concentration of Halon Replacements and Their Function as Fire Suppressants," ACS Symposium Series No. 611, *Halon Replacements: Technology and Science* (A. W. Miziolek and W. Tsang, eds.), The American Chemical Society, 1995, pp. 243-257.

15. Takahashi, F., Schmoll, W. J., and Belovich, V. M., "Suppression of Bluff-Body Stabilized Diffusion Flames," AIAA Paper 98-3529, July 1998.

16. Longwell, J. P., Frost, E. E., and Weiss, M. A., "Flame Stability in Bluff Body Recirculation Zones," *Industrial and Engineering Chemistry* 45: 1629-1637 (1953).

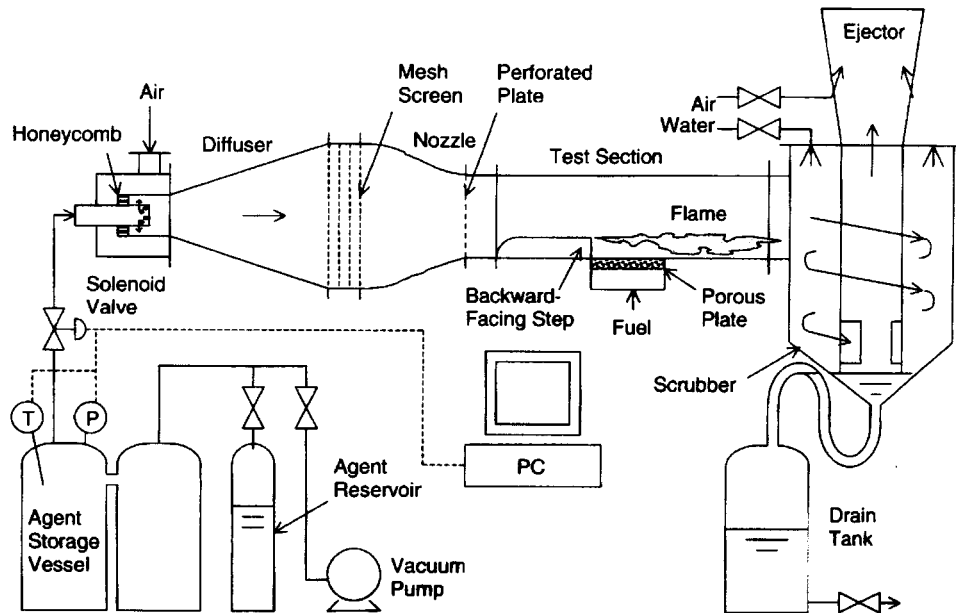


Fig. 1 Experimental apparatus.

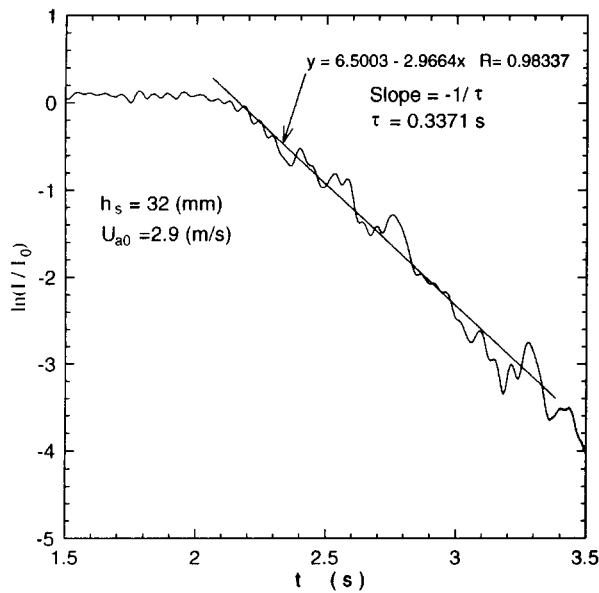


Fig. 2 Sodium D-line emission intensity trace.

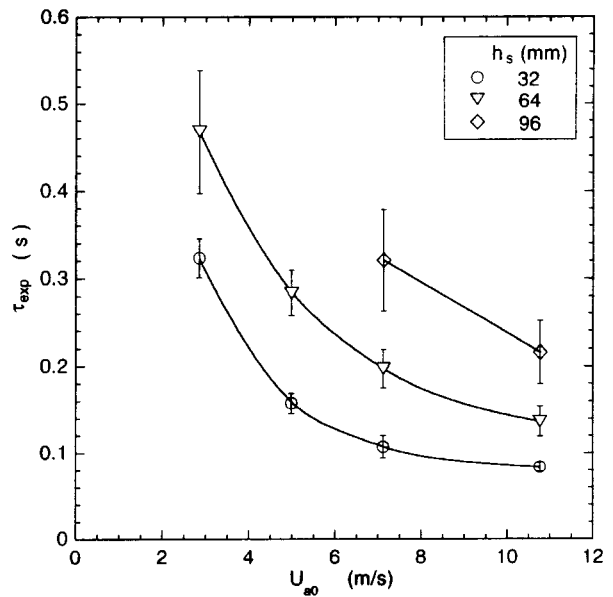


Fig. 3. Measured characteristic mixing time.

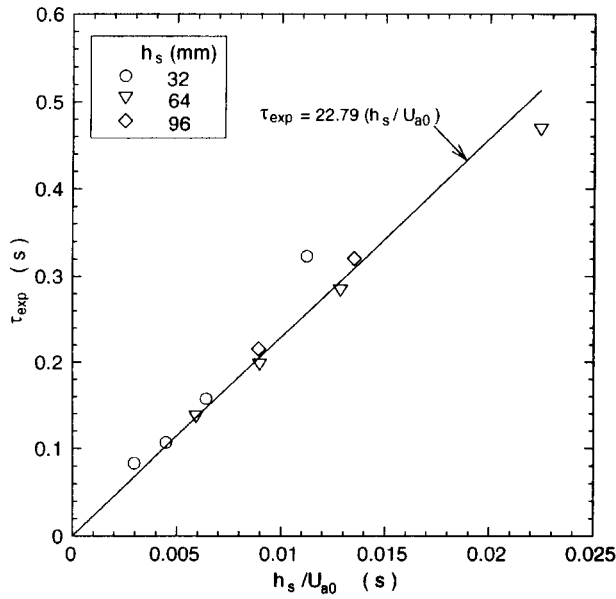


Fig. 4 Correlation between the characteristic mixing time and the step height normalized by the air velocity.

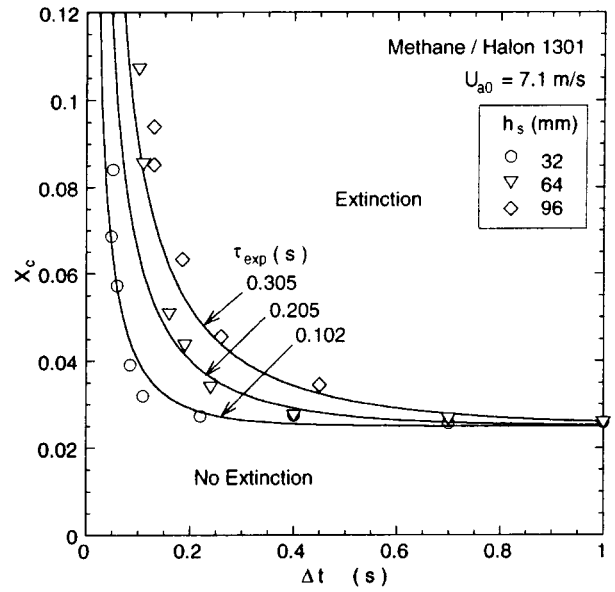


Fig. 6 Measured critical agent mole fraction at suppression and theoretical curves as a function of agent injection period.

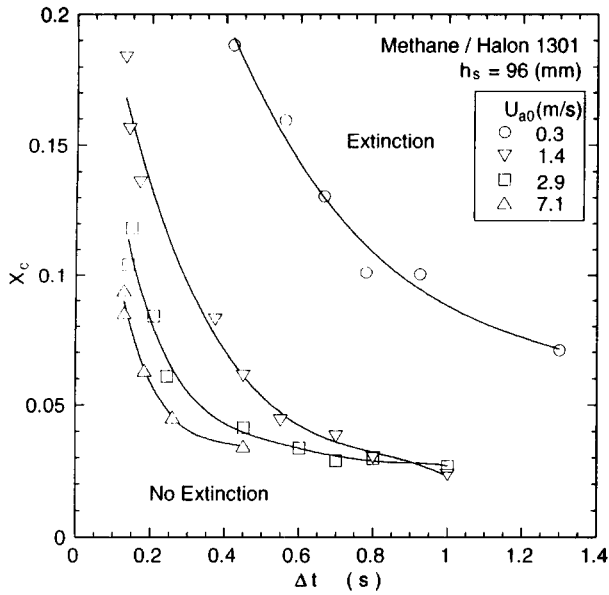


Fig. 5 Measured critical agent mole fraction at suppression as a function of agent injection period.

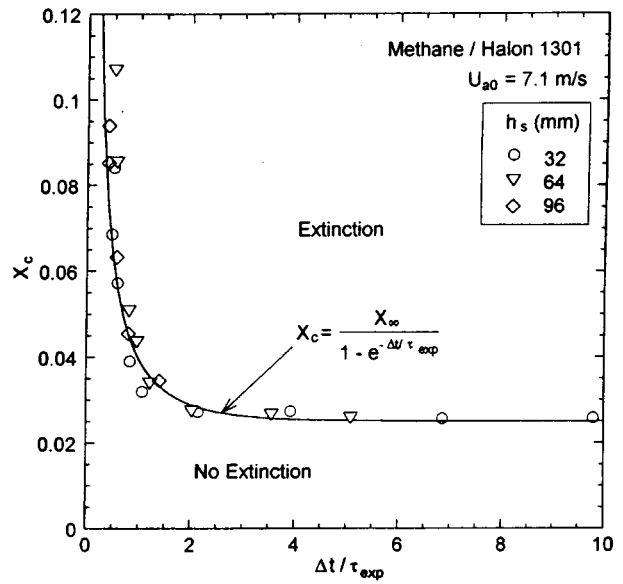


Fig. 7 Measured critical agent mole fraction at suppression and theoretical curves as a function of agent injection period normalized by the characteristic mixing time.

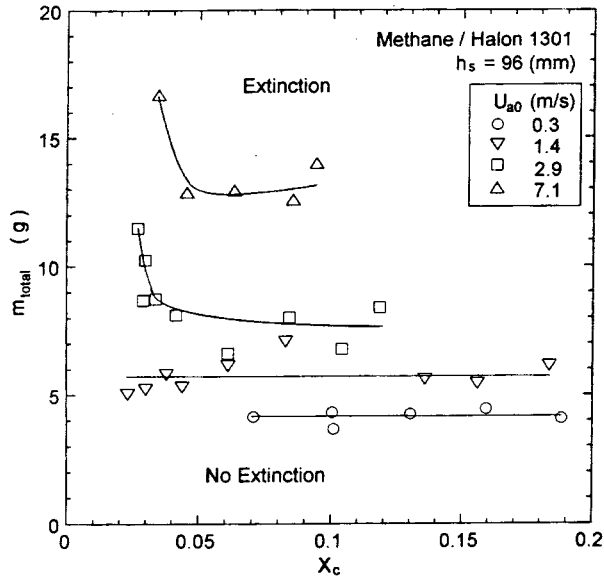


Fig. 8 The total agent mass at suppression as a function of the critical agent mole fraction.

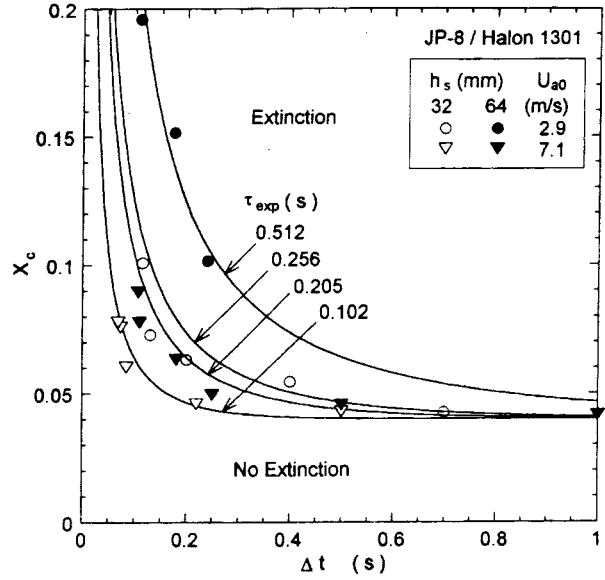


Fig. 10 Measured critical agent mole fraction at suppression as a function of agent injection period.

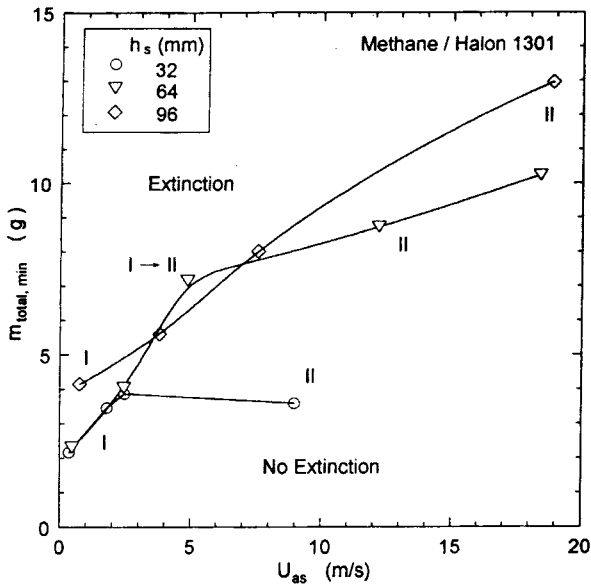


Fig. 9 The minimum total agent mass at suppression as a function of mean air velocity at the step with corresponding flame stabilization and suppression regimes.